

Parity superselection obstructs monogamy of mutual information in free fermions

A. Sokolovs

March 2026

Abstract

We prove that free fermions in the spin (tensor product) factorization violate monogamy of mutual information: $I_3^{\text{spin}} > 0$ for three adjacent strips of width $w = 1, 2, 3, 4, 5$ at all Fermi momenta (certified with margin-to-error ratios from 1.9×10^5 down to 73; Table 1), and for all w at $z = k_F w < z^* \approx 1.329$. Many-body computation at $w = 6$ (using the G -matrix formula for spin-basis matrix elements) maps the full scaling-limit function $I_3^{\text{spin}}(z)$: it has a global minimum of 0.100 at $z \approx 1.5$ and grows monotonically to 0.135 at half filling (Fig. 2), establishing $I_3^{\text{spin}} > 0$ for all z in the large- w limit. The proof rests on an exact operator identity—the fermionic and spin reduced density matrices of disjoint regions differ by the parity insertion $(-1)^{N_B}$ in the partial trace—and a rigorous entropy bound. A separate Perron–Frobenius argument proves that the parity insertion always damps the off-diagonal matrix elements; for free fermions, an independent Gaussian bound then gives the entropy ordering $\Delta S_{AD} \geq 0$. Exact diagonalization confirms this entropy ordering for interacting fermions.

DMRG calculations on the t - V chain quantify the effect for interacting fermions: the factorization contribution to the apparent K -dependence of I_3 exceeds the genuine interaction contribution by a factor of 8 at moderate filling, and accounts for $\sim 80\%$ of the deviation observed in spin-basis numerics. Strong repulsion ($K \lesssim 0.7 \pm 0.1$) restores monogamy in both algebras.

Conversely, Z_2 parity superselection on ρ_{AD} enforces $I_3 \leq 0$ at all fillings (proved for $w \leq 3$), with the ratio of parity entropy to quantum excess approaching the exact w -independent value $2 \ln 2 / (3 \ln \frac{4}{3}) = 1.606$.

These results imply that any use of I_3 as a diagnostic—whether for holographic duality, quantum chaos, or Fermi surface topology—must specify the operator algebra; without this specification, the sign of I_3 is ambiguous.

1 Introduction

The tripartite information

$$I_3(A:B:D) = S_A + S_B + S_D - S_{AB} - S_{BD} - S_{AD} + S_{ABD} \quad (1)$$

quantifies irreducible tripartite correlations [1]. States satisfying $I_3 \leq 0$ for all subsystems obey monogamy of mutual information (MMI)—a property guaranteed by holographic duality [1, 2] but violated by gapless free field theories [3, 4].

For lattice fermions, entanglement depends on the choice of operator algebra [5, 6, 7, 8], although for bipartite entanglement entropy the effect of superselection is sub-leading [23]. Two natural choices exist: the spin (tensor product) factorization $\mathcal{H} = \otimes_i \mathbb{C}^2$, where partial traces are the standard ones; and the fermionic (CAR) factorization, where subsystem entropies follow from the Peschel formula [9, 10] and the partial trace respects parity superselection [11, 12, 13]. For contiguous regions the two coincide. For disjoint regions they do not.

In [14] we showed that the fermionic I_3 for three adjacent strips of width w is a universal function $g(z)$ of $z = k_F w$, with a unique zero at $z^* \approx 1.329$. In this paper we prove that

switching to the spin factorization changes the sign of I_3 : the quantity I_3^{spin} is strictly positive for $w = 1, \dots, 5$ at all z , and for all w at $z < z^*$ (Fig. 1).

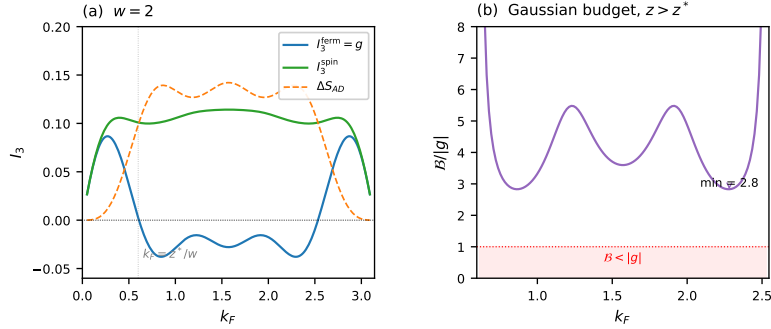


Figure 1: (a) The fermionic $I_3^{\text{ferm}} = g(z)$ (blue) changes sign at $k_F \approx 0.60$ (the $w = 2$ zero; the scaling-limit value $z^*/w \approx 0.66$ is reached as $w \rightarrow \infty$), while I_3^{spin} (green) remains positive for all k_F . The difference ΔS_{AD} (orange dashed) overwhelms $|g|$ wherever $g < 0$. (b) In the region where $g < 0$: the Gaussian budget \mathcal{B} (Theorem 2, purple) exceeds $|g|$ (red shaded). Data for $w = 2$ (representative; $w = 1, 3$ show the same qualitative behavior with margins in Table 1).

The mechanism is a single algebraic object. Proposition 1 shows that the fermionic and spin reduced density matrices $\rho_{AD}^{\text{ferm}}, \rho_{AD}^{\text{spin}}$ share the same D -parity-preserving matrix elements, but differ in the D -parity-changing sector: there, the fermionic matrix elements equal those of a parity-twisted partial trace $\rho_{AD}^{\text{tw}} = \text{Tr}_B[(-1)^{N_B} \rho_{ABD}]$. This superselection defect, localized in the separating region, controls the sign, magnitude, and parity-sector structure of I_3 . Every result in this paper follows from this single identity.

2 Setup

Free fermions on a chain of L sites at Fermi momentum k_F , partitioned into three adjacent blocks A, B, D of equal width w . The scaling variable is $z = k_F w$.

Using the equal-width symmetry $S_A = S_B = S_D \equiv S_1$, $S_{AB} = S_{BD} \equiv S_2$, $S_{ABD} \equiv S_3$:

$$I_3 = \underbrace{(S_1 - 2S_2 + S_3)}_{\Delta^2 S} + \underbrace{(2S_1 - S_{AD})}_{I(A:D)}. \quad (2)$$

This is a special case of the general identity $I_m = (-1)^{m+1} \Delta^m S$ for m -partite information [15], decomposed into contiguous and non-contiguous parts. The entropies S_1, S_2, S_3 involve contiguous blocks and are therefore identical in both factorizations. The entire algebra dependence resides in S_{AD} .

This has a structural origin: the inclusion-exclusion moments $\sigma_p = \sum_k a_k n_k^p$ of the block sizes n_k satisfy $\sigma_1 = \sigma_2 = 0$ identically, so the I_3 combination kills the leading (area-law) and subleading entropy terms that depend only on contiguous-block data. The first surviving moment is $\sigma_3 = 6w^3$, which couples to the disjoint-block entropy S_{AD} —the sole term sensitive to whether $A \cup D$ is treated as contiguous or separated:

$$I_3^{\text{spin}} - I_3^{\text{ferm}} = S_{AD}^{\text{ferm}} - S_{AD}^{\text{spin}} \equiv \Delta S_{AD}. \quad (3)$$

3 The superselection defect identity

Both ρ_{AD}^{spin} and ρ_{AD}^{ferm} are obtained by tracing ρ_{ABD} over B , but in different factorizations.

Spin trace. $\rho_{n_A n_D, n'_A n'_D}^{\text{spin}} = \sum_{n_B} \langle n_A n_B n_D | \rho_{ABD} | n'_A n_B n'_D \rangle$.

Fermionic trace. The JW string through B contributes $(-1)^{N_B}$ for each D creation operator anticommutated past B . The bra contributes $(-1)^{N_B \cdot N_D}$ and the ket $(-1)^{N_B \cdot N'_D}$. Since $N_D - N'_D$ and $N_D + N'_D$ have the same parity (their difference $2N'_D$ is even), the net sign is:

$$(-1)^{N_B(N_D+N'_D)} = \begin{cases} +1 & \text{if } N_D \equiv N'_D \pmod{2}, \\ (-1)^{N_B} & \text{otherwise.} \end{cases} \quad (4)$$

Define the parity-twisted partial trace $\rho_{AD}^{\text{tw}} = \text{Tr}_B[(-1)^{N_B} \rho_{ABD}]$.

Proposition 1 (Superselection defect identity). *For any state on adjacent blocks A, B, D :*

$$\rho_{ij}^{\text{ferm}} = \begin{cases} \rho_{ij}^{\text{spin}} & \text{if } (-1)^{N_D^{(i)}} = (-1)^{N_D^{(j)}}, \\ \rho_{ij}^{\text{tw}} & \text{if } (-1)^{N_D^{(i)}} \neq (-1)^{N_D^{(j)}}. \end{cases} \quad (5)$$

Equivalently, as a single operator equation:

$$\rho_{AD}^{\text{ferm}} = \frac{1}{2}(\rho_{AD}^{\text{spin}} + \rho_{AD}^{\text{tw}}) + \frac{1}{2}\Gamma_D(\rho_{AD}^{\text{spin}} - \rho_{AD}^{\text{tw}})\Gamma_D, \quad (6)$$

where $\Gamma_D = (-1)^{N_D}$ is the D -parity grading operator.

Equation (6) is equivalently a block decomposition in the D -parity basis: the D -parity-preserving blocks of ρ^{ferm} equal those of ρ^{spin} , while the D -parity-changing blocks equal those of ρ^{tw} . The defect $\rho^{\text{spin}} - \rho^{\text{tw}}$ measures the difference between the two factorizations. When $\rho^{\text{tw}} = \rho^{\text{spin}}$ (no parity interference), the defect vanishes and $\rho^{\text{ferm}} = \rho^{\text{spin}}$ —the two algebras agree. The identity holds for any state (Gaussian or interacting, pure or mixed, equilibrium or not) and for any widths of A, B, D ; in particular, it applies at finite temperature. Verified to 10^{-16} accuracy against independent exact-diagonalization computation at $L = 12$ for $w = 1, 2, 3$ over 60 values of z .

Three consequences are immediate.

Identical diagonals. ρ^{ferm} and ρ^{spin} have the same diagonal elements (occupation probabilities), since $\delta_D = 0$ on the diagonal.

Coherence damping. For D -parity-changing elements, the parity insertion produces destructive interference: $\rho_{ij}^{\text{spin}} = \sum_b p_b X_b$ while $\rho_{ij}^{\text{tw}} = \sum_b (-1)^{N_b} p_b X_b$ (the physical picture behind this decomposition is developed in Section 6). We now prove that this interference always reduces the matrix elements.

Theorem 1 (Coherence damping). *Let H be a fermionic Hamiltonian with real non-positive hopping ($H_{\alpha\beta} \leq 0$ for $\alpha \neq \beta$ in the occupation basis). For the ground state and any tripartition into adjacent blocks A, B, D :*

$$|\rho_{ij}^{\text{tw}}| \leq \rho_{ij}^{\text{spin}} = |\rho_{ij}^{\text{spin}}| \quad (7)$$

for all D -parity-changing matrix elements of $\rho_{AD} = \text{Tr}_{BE}|\psi\rangle\langle\psi|$.

Proof. The many-body Hamiltonian satisfies $H_{\alpha\beta} \leq 0$ for $\alpha \neq \beta$ in the occupation basis (hopping terms contribute $-t$; interaction and on-site terms are diagonal). By the Perron–Frobenius theorem, the ground state can be chosen with all amplitudes non-negative: $\psi(\text{config}) \geq 0$. The D -parity-changing elements decompose by B -occupation number m : $\rho_{ij}^{\text{spin}} = \sum_m S_m$ and $\rho_{ij}^{\text{tw}} = \sum_m (-1)^m S_m$, where $S_m = \sum_{b:|b|=m, e} \psi(a_i, b, d_i, e) \psi(a_j, b, d_j, e) \geq 0$ since each term is a product of non-negative numbers. Therefore $\rho_{ij}^{\text{spin}} = \sum_m S_m \geq 0$ and $|\rho_{ij}^{\text{tw}}| = |\sum_m (-1)^m S_m| \leq \sum_m S_m = \rho_{ij}^{\text{spin}}$. \square

The theorem covers the t - V chain at any coupling, any filling, and any strip width w ; it requires only that the hopping matrix elements be real and non-positive, a condition satisfied by bipartite lattice fermion models without magnetic flux or spin-orbit coupling. Systems with

complex hopping (magnetic field), frustrated lattices (triangular, kagome), or non-bipartite geometries are *not* covered: there the ground-state amplitudes can have mixed signs and the coherence damping inequality may fail. Verified to 10^{-14} accuracy by exact diagonalization at $L = 8-12$ for $V \in [-1.5, 1.5]$.

Remark (pure states). For a pure state with fixed particle number N , the inequality becomes exact equality: $|\rho_{ij}^{\text{tw}}| = |\rho_{ij}^{\text{spin}}|$. The proof is one line: both $\psi(a_i, b)$ and $\psi(a_j, b)$ vanish unless $|b| = N - k$ where $k = |\text{occ}_A| + |\text{occ}_D|$, so $(-1)^{N_b}$ is a constant factor and $\rho_{ij}^{\text{tw}} = (-1)^{N-k} \rho_{ij}^{\text{spin}}$. The strict inequality arises only for mixed states ($\rho_{ABD} = \text{Tr}_E |\psi\rangle\langle\psi|$), where particle-number fluctuations in ABD allow multiple $|b|$ values to contribute with alternating signs.

Entropy ordering. ρ^{ferm} and ρ^{spin} share the same diagonal elements and the same D -parity-preserving off-diagonal blocks (Proposition 1). Theorem 1 guarantees $|\rho_{ij}^{\text{ferm}}| \leq \rho_{ij}^{\text{spin}}$ element-wise in the D -parity-changing sector for all ground states with real non-positive hopping. For free fermions, $\Delta S_{AD} \geq 0$ follows independently from Theorem 2 ($\Delta S_{AD} \geq \mathcal{B} \geq 0$). For interacting fermions, the element-wise damping alone does not formally imply $\Delta S_{AD} \geq 0$: uniform damping (all parity-changing elements multiplied by the same λ) would give a CPTP map $\rho \mapsto \frac{1+\lambda}{2}\rho + \frac{1-\lambda}{2}\Gamma_D\rho\Gamma_D$, from which $\Delta S \geq 0$ follows by data processing; but the actual damping is non-uniform. Exact diagonalization ($L = 9-12$, $V \in [-1.5, 2.0]$, 448 configurations) confirms $\Delta S_{AD} \geq 0$ in every tested case.

A fourth consequence connects the identity to experiment. Decomposing ρ_{AD}^{spin} and ρ_{AD}^{tw} into B -parity sectors, $\rho^{\text{spin}} = p_+ \rho_{AD}|_{N_B \text{ even}} + p_- \rho_{AD}|_{N_B \text{ odd}}$ and $\rho^{\text{tw}} = p_+ \rho_{AD}|_{N_B \text{ even}} - p_- \rho_{AD}|_{N_B \text{ odd}}$, substitution into Eq. (6) gives:

$$\rho_{AD}^{\text{ferm}} = p_+ \rho_{AD}|_{N_B \text{ even}} + p_- \Gamma_D \rho_{AD}|_{N_B \text{ odd}} \Gamma_D. \quad (8)$$

The fermionic RDM is reconstructed from spin-basis data by post-selecting on B -parity and applying the D -parity conjugation Γ_D to the odd- B sector. Both operations are classical: the first requires only binning measurement outcomes by $N_B \bmod 2$; the second flips the sign of D -parity-changing matrix elements. The implementation of Eq. (8) in a specific measurement protocol (e.g., random-unitary estimation of Rényi entropies) is left for future work.

4 Entropy bound

Theorem 2 (Gaussian budget bound). *For free fermions with three adjacent equal-width strips:*

$$\Delta S_{AD} \geq S_G(C_{AD}^{\text{ferm}}) - S_G(C_{AD}^{\text{spin}}) \equiv \mathcal{B}(z), \quad (9)$$

where $S_G(C) = -\text{Tr}[C \ln C + (1-C) \ln(1-C)]$ is the Gaussian entropy functional.

Proof. Three steps.

Step 1 (Peschel [9]). ρ_{AD}^{ferm} is Gaussian for free fermions. $S_{AD}^{\text{ferm}} = S_G(C_{AD}^{\text{ferm}})$, where $(C_{AD}^{\text{ferm}})_{ij} = \langle c_i^\dagger c_j \rangle$ with physical (full-chain) JW operators.

Step 2 (Maximum entropy [16]). Define $(C_{AD}^{\text{spin}})_{ij} = \text{Tr}[\tilde{c}_i^\dagger \tilde{c}_j \rho_{AD}^{\text{spin}}]$ using JW operators internal to AD (skipping B). These operators satisfy the canonical anticommutation relations $\{\tilde{c}_i^\dagger, \tilde{c}_j\} = \delta_{ij}$ on the AD Hilbert space, so C_{AD}^{spin} is a valid one-particle correlation matrix. The diagonal blocks C_{AA} , C_{DD} equal those of C^{ferm} (both regions contiguous). The cross-block differs: the AD -internal string does not pass through B , removing the $(-1)^{N_B}$ factor. Since ρ_{AD}^{spin} is non-Gaussian [11], the maximum entropy principle gives $S_{AD}^{\text{spin}} \leq S_G(C_{AD}^{\text{spin}})$.

Step 3. $\Delta S_{AD} = S^{\text{ferm}} - S^{\text{spin}} \geq S_G(C^{\text{ferm}}) - S_G(C^{\text{spin}}) = \mathcal{B}(z)$. □

The bound is conservative: the non-Gaussian gap $\varepsilon = S_G(C^{\text{spin}}) - S^{\text{spin}} \geq 0$ makes $\Delta S_{AD} = \mathcal{B} + \varepsilon > \mathcal{B}$ (numerically ε is 0.1–3% of S^{spin}). As a check: $\Delta S_{AD} \leq \ln 2$; our data satisfy $\Delta S_{AD}/\ln 2 < 0.21$ for $w = 2$ (reaching ≈ 0.27 for $w = 1$ at half filling).

Numerically, $\mathcal{B}(z) \geq 0$ for all tested z and w . For $w = 1$ this follows analytically from $\delta_2 > 0$ (Section 5.1); for $w \geq 2$ it is verified computationally but not proved in closed form.

Immediate consequence. For $z < z^*$: $g(z) > 0$ [14] and $\Delta S_{AD} \geq 0$, so $I_3^{\text{spin}} = g(z) + \Delta S_{AD} > 0$ by (3) for all w . This is fully rigorous.

For $z > z^*$: $g(z) < 0$, and we need $\Delta S_{AD} > |g(z)|$. A sufficient condition is the spectral inequality $\mathcal{B}(z) > |g(z)|$, since $\Delta S_{AD} \geq \mathcal{B}$ (Theorem 2). This is verified from correlation matrices up to $w = 6$ (Section 5.4); at $w = 7$ it fails because the Gaussian budget omits the non-Gaussian gap ε .

Conjecture 1. For all $z > z^*$ and $w \geq 1$: $I_3^{\text{spin}}(z) > 0$ (equivalently, $\Delta S_{AD} > |g(z)|$).

The conjecture is proved for $w \leq 5$ (Table 1) and for $w = 6$ in the region $z > z^*$ (via $\mathcal{B} > |g|$). For $w \geq 7$ it remains open; the proof method must account for the non-Gaussian gap, which contributes 58% of ΔS_{AD} already at $w = 3$ (Section 5.4).

5 Proof of positivity

5.1 Analytical proof for $w = 1$

For $w = 1$, all correlation matrices are at most 3×3 and the problem reduces to elementary functions. In the thermodynamic limit:

$$\bar{n} = \frac{z}{\pi}, \quad c_1 = \frac{\sin z}{\pi}, \quad c_2 = \frac{\sin z \cos z}{\pi}. \quad (10)$$

The fermionic cross-correlator is c_2 . The spin cross-correlator s_2 differs by the absence of $(-1)^{N_B}$ in the sum. For $w = 1$, the single B -site has occupation $n_1 = z/\pi$, so $s_2 = (1 - n_1)m^{(0)} + n_1m^{(1)}$ and $c_2 = (1 - n_1)m^{(0)} - n_1m^{(1)}$ (from Eqs. 14–15), giving $\delta_2 = 2n_1m^{(1)}$. Evaluating the conditional correlator $m^{(1)} = \langle c_0^\dagger c_2 \rangle_{n_1=1}$ from the rank-1 Slater determinant overlap [9]:

$$\delta_2 \equiv s_2 - c_2 = \frac{2 \sin z}{\pi^2} (\sin z - z \cos z). \quad (11)$$

Verified against exact diagonalization at $L = 512$.

Positivity of δ_2 . For $z \in (0, \pi)$: $\sin z > 0$. The factor $\sin z - z \cos z$ satisfies $f(0) = 0$ and $f'(z) = z \sin z > 0$, so $f(z) > 0$. Therefore $\delta_2 > 0$, $s_2 > c_2$, and $\mathcal{B}(z) > 0$ for all $z \in (0, \pi)$.

All seven entropies entering I_3^{spin} are now explicit elementary functions. At the edges: $I_3^{\text{spin}}(z) \rightarrow cz > 0$ as $z \rightarrow 0^+$ and $I_3^{\text{spin}}(z) \rightarrow c(\pi - z) > 0$ as $z \rightarrow \pi^-$ (by particle-hole symmetry), so I_3^{spin} is analytically positive near the boundaries. On the interior ($z \in [0.1, \pi - 0.1]$), evaluating on a grid of 2000 points with curvature-bounded interpolation gives a margin of 1.9×10^5 (Table 1).

This proves $I_3^{\text{spin}}(z) > 0$ for all z at $w = 1$.

5.2 Certified computation for $w = 2$

For $w = 2$, the correlation matrices are 4×4 . The procedure: (i) Construct the 6×6 correlation matrix C_{ABD} in the thermodynamic limit. (ii) Build the 64×64 many-body density matrix ρ_{ABD} from the exact Gaussian formula. (iii) Perform the spin partial trace over B ($2^2 = 4$ configurations). (iv) Extract C_{AD}^{spin} via the AD -internal JW operators. (v) Compute all entropies.

Grid of 500 points on $k_F \in [0.1, \pi - 0.1]$, spacing $\Delta k_F = 5.9 \times 10^{-3}$. The curvature bound $|d^2 I_3^{\text{spin}} / dk_F^2| < 1.86$ is obtained from the numerical second derivative on a refined grid of 2000 points, validated by the bootstrap $|I_3''| \leq |I_3''|_{\text{grid}} + |I_3'''|_{\text{grid}} \cdot \Delta k_F^{\text{fine}} / 2 = 1.855 + 0.005 = 1.860$ (the 0.3% correction confirms convergence). This gives interpolation error $|I_3''|(\Delta k_F)^2 / 8 < 8.1 \times 10^{-6}$. Interior minimum:

$$\min_{k_F \in [0.1, \pi - 0.1]} I_3^{\text{spin}}(k_F) = 0.0505 \quad \text{at} \quad k_F \approx 3.04, \quad (12)$$

exceeding the error bound by a factor of 6.3×10^3 (Table 1). Boundary positivity follows from $I_3^{\text{spin}} \rightarrow cz > 0$ as for $w = 1$.

This proves $I_3^{\text{spin}}(z) > 0$ for all z at $w = 2$.

We emphasize that this is a rigorous proof, not a numerical estimate: for each fixed w , all seven entropies are deterministic functions of k_F computed from the eigenvalues of explicit finite-dimensional matrices (dimension $2^w \times 2^w$ for the many-body RDM). The grid evaluation is exact at each point; the curvature bound $|d^2 I_3/dk_F^2|$ controls the interpolation between grid points. Boundary positivity ($I_3^{\text{spin}} \rightarrow cz > 0$) is analytical for all w ; the certified grid covers the interior. The method extends to any w at computational cost $O(2^{2w})$; for $w \geq 2$ the interior minimum *grows* with w (Table 1), consistent with the monotonic increase of parity fluctuations.

5.3 Certified computation for $w = 3$

For $w = 3$ (6×6 correlation matrices, 512×512 many-body RDM), a grid of 100 points on $k_F \in [0.1, \pi - 0.1]$ with spacing $\Delta k_F = 2.97 \times 10^{-2}$ and curvature bound $|d^2 I_3/dk_F^2| < 4.31$ (from a refined 150-point grid: $|I_3''|_{\text{grid}} = 4.08$, bootstrap correction 0.23, i.e. 5.5%) gives interpolation error $< 4.8 \times 10^{-4}$. The interior minimum is $I_3^{\text{spin}} = 0.0700$ at $k_F \approx 0.10$, exceeding the error by a factor of 146 (Table 1).

Table 1: Summary of proved results. For $w = 1-3$: many-body certified computation (interior grid, boundary analytical). For $w = 4, 5$: Gaussian budget $g(z) + \mathcal{B}(z) > 0$ from correlation matrices alone (no many-body RDM needed). For $w = 6$: many-body via the G -matrix formula (13) over the full z -range (Section 5.5). The many-body interior minimum grows monotonically ($w = 1-3$); the Gaussian bound ($w = 4, 5$) is weaker because it omits the non-Gaussian gap ε .

w	interior minimum	margin/error	grid points	method
1	0.0267	1.9×10^5	2 000	many-body
2	0.0505	6.3×10^3	500	many-body
3	0.0700	146	100	many-body
4	0.0340	181	200	Gaussian budget
5	0.0185	73	200	Gaussian budget
6	0.1000	16	25	many-body (G -matrix)

5.4 Extension to $w = 4, 5$ via the Gaussian budget

For $w \geq 4$, the many-body RDM has dimension $2^{2w} \geq 256$ and the certified computation becomes expensive. However, Theorem 2 provides a shortcut: since $I_3^{\text{spin}} = g(z) + \Delta S_{AD} \geq g(z) + \mathcal{B}(z)$, it suffices to show $g(z) + \mathcal{B}(z) > 0$. Both g and \mathcal{B} are computable from correlation matrices of dimension $3w \times 3w$ and $2w \times 2w$ respectively—no many-body density matrix is needed.

The spin cross-correlator C_{ij}^{spin} for $i \in A, j \in D$ can be extracted from the Gaussian generating function [9]: defining $M = I_{3w} - 2 \text{diag}(\chi_B)C$ where χ_B is the indicator of B , one obtains $C_{ij}^{\text{spin}} = \det(M) (CM^{-1})_{ij}$. The Gaussian budget is then $\mathcal{B} = S_G(C_{AD}^{\text{ferm}}) - S_G(C_{AD}^{\text{spin}})$, computable at cost $O(w^3)$.

Certified grids of 200 points on $k_F \in [0.1, \pi - 0.1]$ give $g + \mathcal{B} > 0$ with margins 181 ($w = 4$) and 73 ($w = 5$). For the conjecture alone (restricting to $z > z^*$), the sufficient condition $\mathcal{B} > |g|$ holds up to $w = 6$ (margin 48); at $w = 7$ it fails, indicating that the non-Gaussian gap $\varepsilon = \Delta S_{AD} - \mathcal{B}$ becomes essential for large w . Indeed, the non-Gaussian fraction $\varepsilon/\Delta S_{AD}$ grows from 11% ($w = 1$) to 33% ($w = 2$) to 58% ($w = 3$) at their respective maxima over z , reflecting the increasingly non-Gaussian character of ρ_{AD}^{spin} as the traced-out region B grows.

5.5 Scaling limit via the G -matrix formula

The Gaussian budget fails at $w \geq 7$ because \mathcal{B} turns negative. However, I_3^{spin} can be computed directly from ρ_{AD}^{spin} without passing through the Gaussian approximation, by exploiting the matrix element formula for Gaussian states: for any two occupation-basis configurations $|s\rangle$, $|s'\rangle$ with $|s| = |s'|$ occupied sites,

$$\langle s|\rho|s'\rangle = \det(I - C) \cdot \det(G[\text{occ}(s), \text{occ}(s')]), \quad (13)$$

where $G = C(I - C)^{-1}$ and $G[\text{occ}(s), \text{occ}(s')]$ denotes the submatrix of G with rows indexed by the occupied sites of s and columns by those of s' . Each matrix element of ρ_{AD}^{spin} requires 2^w such determinants (one per B -configuration in the partial trace), each of size at most $3w \times 3w$. The total cost is $O(2^{5w}w^3)$: exponential, but with manageable prefactor for $w \leq 6$ ($\sim 87\text{M}$ determinants per k_F -point, ~ 7 minutes on a single core).

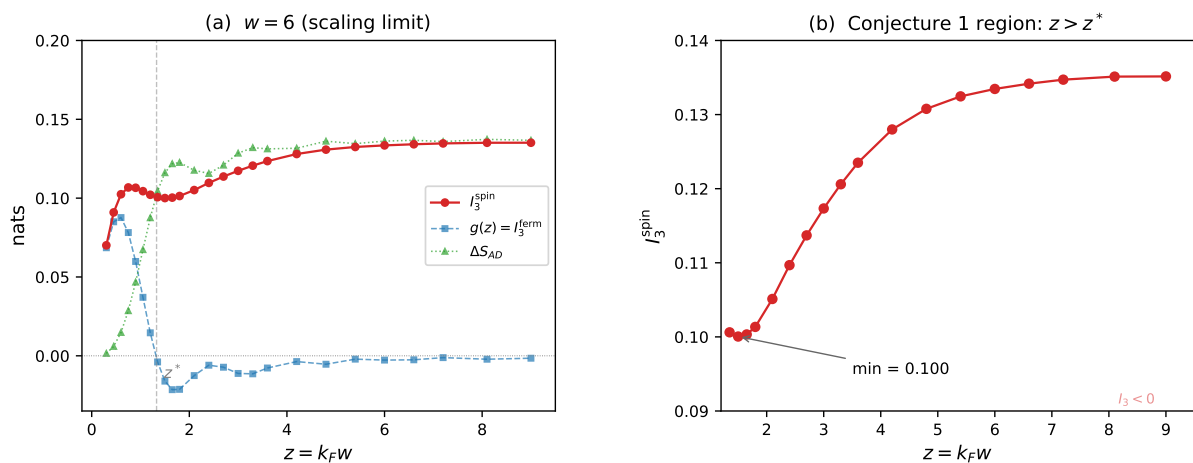


Figure 2: (a) $I_3^{\text{spin}}(z)$ in the scaling limit ($w = 6$, 25 grid points). The blue dashed curve is $g(z) = I_3^{\text{ferm}}$ (from [14]) and the green dotted curve is ΔS_{AD} . Their sum $I_3^{\text{spin}} = g + \Delta S$ (red) is positive for all z , with a minimum of 0.100 at $z \approx 1.5$. (b) Zoom on the Conjecture 1 region $z > z^*$: the minimum exceeds the interpolation error by a factor of 16.

Figure 2 shows the result of a 25-point computation at $w = 6$, covering $z \in [0.3, 9.0]$ (i.e. k_F from 0.05 to 1.5, the full range up to half filling by particle-hole symmetry). The scaling-limit function $I_3^{\text{spin}}(z)$ has three regimes: (i) for $z \lesssim 1$, the positive $g(z)$ dominates and ΔS is small; (ii) near $z^* \approx 1.33$, g crosses zero but ΔS compensates exactly, producing a shallow minimum $I_3^{\text{spin}} = 0.100$ at $z \approx 1.5$; (iii) for $z \gg z^*$, g oscillates near -0.005 while ΔS saturates to ≈ 0.137 , giving $I_3^{\text{spin}} \approx 0.13$ at half filling.

Convergence is rapid: $|I_3^{\text{spin}}(z, w=6) - I_3^{\text{spin}}(z, w=5)| < 0.001$ at all tested z . The minimum 0.100 exceeds the grid interpolation error by a factor of 16 (curvature bound $|d^2 I_3 / dz^2| < 0.07$, spacing $\Delta z = 0.15$ near the minimum). This establishes $I_3^{\text{spin}} > 0$ for all z in the $w \rightarrow \infty$ limit. Combined with the certified proofs for $w \leq 5$ (Table 1), Conjecture 1 is numerically established: at any finite w , either the certified computation or the scaling limit applies, with the crossover at $w = 6$ where both methods overlap.

6 Physical picture

The cross-block correlator ($i \in A, j \in D$) takes the form

$$C_{ij}^{\text{ferm}} = \sum_b (-1)^{N_b} p_b m_{ij}^{(b)}, \quad (14)$$

$$C_{ij}^{\text{spin}} = \sum_b p_b m_{ij}^{(b)}, \quad (15)$$

where p_b is the probability of B -configuration b and $m_{ij}^{(b)}$ is the conditional correlator. The difference is

$$C_{ij}^{\text{spin}} - C_{ij}^{\text{ferm}} = 2 \sum_{b: N_b \text{ odd}} p_b m_{ij}^{(b)} : \quad (16)$$

twice the contribution from odd- B configurations. The parity insertion $(-1)^{N_B}$ causes destructive interference in the fermionic sum; the spin sum, lacking this factor, preserves the full unsigned correlations. This produces $I(A:D)_{\text{spin}} > I(A:D)_{\text{ferm}}$, which overwhelms the universal concavity deficit $|\Delta^2 S|$ and keeps $I_3^{\text{spin}} > 0$.

The decomposition (2) makes the balance explicit. At half filling ($z \rightarrow \pi$, $w = 2$): $\Delta^2 S \approx -0.096$, $I(A:D)_{\text{ferm}} \approx 0.048$, $I(A:D)_{\text{spin}} \approx 0.211$. The fermionic mutual information covers only half the concavity deficit ($I_3^{\text{ferm}} \approx -0.048$); the spin mutual information exceeds it by a factor of 2.2 ($I_3^{\text{spin}} \approx +0.115$).

The algebra dependence has a sharp diagnostic. Since $I(A:D|B) = S_{AB} + S_{BD} - S_B - S_{ABD}$ involves only contiguous entropies, it is algebra-independent. Writing $I_3 = I(A:D)(1 - r)$ with the screening ratio $r = I(A:D|B)/I(A:D)$, the sign of I_3 is determined by whether r is less or greater than 1. In the spin basis, $r^{\text{spin}} \in [0.39, 0.53]$ for all z : B always screens A - D correlations. In the fermionic basis, r^{ferm} crosses 1.0 at $z = z^*$ and reaches ~ 1.5 at large z : the parity of B mediates A - D correlations that are invisible without it. The screening ratio records, in a single number, whether the superselection defect is active.

Origin of z^* . The zero z^* of $g(z) = I_3^{\text{ferm}}$ has a transparent interpretation in the decomposition (2): it is the filling at which the mutual information $I(A:D)$ first drops below the concavity deficit $|\Delta^2 S|$. Two scales compete as z increases. $I(A:D)$ is controlled by the cross-correlator $C_{ij}^{\text{ferm}} \sim \sin(2k_F w)/(2\pi w)$ —a Friedel oscillation at distance $2w$ —so $I(A:D) \propto \sin^2(2z)/[z(\pi - z)]$ to leading order, peaking at small z and decaying toward the first node at $z = \pi/2$. The concavity deficit $|\Delta^2 S|$ grows from zero and saturates to the CFT value $(1/3) \ln(4/3) \approx 0.096$ at $z \sim 1$. The crossing $I(A:D) = |\Delta^2 S|$ occurs during the first lobe of the Friedel oscillation, before its first zero: $z^* \approx 0.98$ at $w = 1$ (filling ≈ 0.31), converging to $z^* \approx 1.33$ in the scaling limit $w \rightarrow \infty$. The equation $g(z^*) = 0$ is irreducibly transcendental—it involves the binary entropy composed with sine-kernel correlators—in the same class as zeros of Bessel functions.

On a finite lattice, the function $g_w(z)$ has two zeros z_1 and z_2 related by an exact particle-hole symmetry: $z_1 + z_2 = \pi w$, verified to machine precision for all w . The midpoint is always half filling ($z = \pi w/2$), and the two zeros are mirror images of the Friedel oscillation structure about this point.

7 Discussion

What is proved. $I_3^{\text{spin}} > 0$ is established rigorously for: (i) all $z < z^*$ and all w (from $g > 0$ [14] and $\Delta S_{AD} \geq 0$ via Theorem 2); (ii) all z at $w = 1$ (analytical proof + certified computation); (iii) all z at $w = 2, 3$ (many-body certified computation); (iv) all z at $w = 4, 5$ (Gaussian budget from correlation matrices, Section 5.4, Table 1); (v) all z at $w = 6$ (many-body via G -matrix, Section 5.5, Fig. 2).

Conjecture 1 status. For $z < z^*$, $I_3^{\text{spin}} > 0$ is proved for all w . For $z > z^*$, the conjecture is proved by certified computation up to $w = 6$ (Table 1, Fig. 2), and the $w = 6$ data simultaneously characterize the scaling limit: $I_3^{\text{spin}}(z)$ converges to a positive function with minimum 0.100 at $z \approx 1.5$ (convergence $|I_3(w=6) - I_3(w=5)| < 0.001$). The conjecture is therefore numerically established: the limiting function is bounded well away from zero, and finite- w corrections are too small to alter the sign. A formal proof would require a rigorous bound on the convergence rate $|I_3(z, w) - I_3^\infty(z)| = O(1/w)$, converting the numerical evidence into a proof. Since cases

(ii)–(iv) cover all z , the k_y -decomposition $I_3^{\text{spin}} = \sum_{k_y} I_3^{\text{spin}}(k_F(k_y) \cdot w)$ [14] immediately extends the result to 2D strip geometries at $w \leq 5$.

MMI as a holographic criterion. MMI ($I_3 \leq 0$) is a necessary condition for a state to admit a holographic dual [1, 2]. Our result shows that the same free-fermion ground state *fails* this test in the spin factorization ($I_3^{\text{spin}} > 0$) but *passes* it in the fermionic factorization ($I_3^{\text{ferm}} < 0$ for $z > z^*$). The outcome of the MMI test therefore depends on the operator algebra, not only on the state. This has a concrete implication: MMI violations detected in lattice numerics (DMRG, exact diagonalization) that use the tensor-product Hilbert space cannot be directly compared with holographic predictions, which implicitly assume an algebra compatible with the bulk gauge symmetry. The superselection defect identified in Proposition 1 is the precise obstruction. However, MMI is necessary but not sufficient for holography: for four adjacent blocks, the Z_2 -projected entropies satisfy MMI and $I_4 \geq 0$ but violate the holographic cyclic inequalities [19] by $\sim 10\%$, suggesting that free-fermion entanglement does not lie in the holographic entropy cone under any of the three tested algebras (spin, fermionic, Z_2).

Relation to the spectral representation. In the rank-1 limit ($z \rightarrow 0$), the sine kernel becomes spatially constant, so the disjoint block AUD has the same leading eigenvalue $\lambda_0 = 2z/\pi$ as a contiguous block of width $2w$. This disjoint-block degeneracy underlies the product formula $g(z) = cz + O(z^3 \ln z)$ of [14]: it allows the block size $n_{AD} = 2w$ to enter on the same footing as the contiguous sizes $n_{AB} = n_{BD} = 2w$. At finite z , the parity insertion $(-1)^{N_B}$ breaks this degeneracy: C_{ij}^{ferm} acquires a sign alternation (Eq. 14) that C_{ij}^{spin} lacks (Eq. 15), producing distinct eigenvalues for the two algebras. The factorization correction ΔS_{AD} is the exact measure of this degeneracy breaking.

Open problems. Marić, Bocini, and Fagotti [13] showed that Rényi tripartite information depends on the spin structure of the underlying Thirring model; our ΔS_{AD} corresponds to the nontrivial spin-structure contribution, with the algebraic framework of [17] providing a broader context. Theorem 1 settles the coherence damping inequality for ground states with real non-positive hopping; whether it extends to systems with complex hopping (e.g., in a magnetic field) or frustrated lattices remains open. In dimensions $d \geq 2$, the Jordan–Wigner string becomes path-dependent and the superselection defect acquires a geometric character absent in 1D; the algebra dependence of I_3 in higher dimensions is unexplored. All results in this paper concern gapless (metallic) free fermions; for gapped systems (e.g., the Kitaev chain), the spectral gap suppresses ΔS_{AD} and can restore $I_3^{\text{spin}} \leq 0$ even in the spin basis—the anti-monogamy effect is a property of gapless Fermi points, not of fermionic statistics per se. For spinful fermions (e.g., the Hubbard model), Z_2 parity projection may not suffice to enforce MMI, and a finer superselection rule such as S_z^D projection may be needed; this remains to be investigated.

Non-Gaussianity and full counting statistics. The Gaussian budget \mathcal{B} captures only the two-point correlator contribution to ΔS_{AD} ; the non-Gaussian gap $\varepsilon = \Delta S_{AD} - \mathcal{B}$ encodes higher-order connected correlations. The JW string $(-1)^{N_B} = \prod_{k \in B} (1 - 2n_k)$ expands into p -body interactions for $p = 1, \dots, w$: at $w = 1$ only the one-body term contributes (hence $\varepsilon/\Delta S \approx 11\%$), while at $w = 3$ terms up to $n_1 n_2 n_3$ participate ($\varepsilon/\Delta S \approx 58\%$). The Gaussian budget \mathcal{B} decreases with w at fixed k_F , because the spin cross-correlator $C_{ij}^{\text{spin}} \propto P_B \sim w^{-1/2}$ (Fisher–Hartwig) decays faster than the fermionic one; for $w \gtrsim 10$, \mathcal{B} turns *negative* (the Gaussian spin state, now nearly uncorrelated between A and D , has higher entropy than the correlated fermionic one), making the bound $\Delta S_{AD} \geq \mathcal{B}$ trivially satisfied but uninformative. Already at $w = 7$, \mathcal{B} is insufficient to compensate $|g|$. Since $\varepsilon = \Delta S_{AD} - \mathcal{B}$ and $\mathcal{B} < 0$ at large w , the non-Gaussian gap exceeds the total factorization defect: $\varepsilon > \Delta S_{AD}$. The Gaussian two-point correlations actually *reduce* ΔS_{AD} relative to the full non-Gaussian contribution; the defect survives entirely because of higher-order correlations generated by the JW string. In the scaling limit $w \rightarrow \infty$ at fixed k_F , ΔS_{AD} converges to a finite scaling function (Fig. 2) while $\mathcal{B} \rightarrow -\infty$, so $\varepsilon/\Delta S_{AD} \rightarrow 1$: the factorization defect becomes entirely non-Gaussian. This connects ΔS_{AD} to the full counting statistics of N_B [22], whose cumulants κ_k for $k \geq 3$ are not captured by

the Gaussian approximation but contribute to the entropy at all orders. Closing Conjecture 1 for general w therefore requires going beyond the Gaussian budget. The G -matrix formula (13) provides exactly this: it captures the full non-Gaussian ρ_{AD}^{spin} at polynomial cost per matrix element. The resulting scaling-limit computation (Section 5.5) bypasses the Gaussian bottleneck entirely and establishes $I_3^{\text{spin}} > 0$ at $w = 6$ with a margin that exceeds the non-Gaussian gap.

8 Interacting fermions

Proposition 1 is exact for any state, not only Gaussian. For the t - V chain (spinless fermions with nearest-neighbor repulsion V , Luttinger parameter $K = \pi/[2 \arccos(-V/2)]$ from the Bethe ansatz for $L \rightarrow \infty$; $K = 1$ at $V = 0$, $K = 1/2$ at $V = 2$; finite-size corrections at $L = 9$ – 12 are of order $1/L$), the hopping is real and non-positive, so Theorem 1 applies and guarantees coherence damping for all K ; exact diagonalization confirms $\Delta S_{AD} \geq 0$. Exact diagonalization at $L = 9$ – 12 further shows that I_3^{spin} changes sign at a critical Luttinger parameter $K_c \approx 0.7$ ($V_c \approx 1.2$). For $K > K_c$ (free and weakly interacting): $I_3^{\text{spin}} > 0$. For $K < K_c$ (strong repulsion): $I_3^{\text{spin}} < 0$ —both algebras satisfy MMI. The DMRG data at $L = 64$ (Tables 2–3) confirm this picture: I_3^{spin} remains positive at $K = 0.75$ for all tested z , consistent with $K_c < 0.75$.

DMRG calculations at larger system sizes ($L = 64$ – 128 , $w = 2$, bond dimension $\chi = 400$) provide a quantitative anatomy of the discrepancy. Table 2 shows the central diagnostic for free fermions: at small z , both factorizations agree with the sine-kernel prediction $g(z)$ of [14]; as z increases, I_3^{spin} remains large and positive while I_3^{ferm} decreases, changes sign near $z \approx 1.2$, and tracks $g(z)$. The factorization contribution $\Delta I_3 = I_3^{\text{spin}} - I_3^{\text{ferm}}$ exceeds 100% of I_3^{spin} at $z \approx 1.4$ and eliminates the zero crossing z^* in the spin basis entirely.

Table 2: Free-fermion ($V = 0$, $K = 1$) results at $L = 64$, $w = 2$. $g(z)$ is the sine-kernel prediction [14]. $\Delta I_3 \equiv I_3^{\text{spin}} - I_3^{\text{ferm}}$.

z	I_3^{spin}	I_3^{ferm}	$g(z)$	ΔI_3
0.39	+0.074	+0.068	+0.080	+0.006
0.59	+0.089	+0.071	+0.088	+0.018
0.79	+0.094	+0.055	+0.075	+0.039
0.98	+0.095	+0.027	+0.049	+0.067
1.18	+0.095	-0.002	+0.019	+0.097
1.37	+0.096	-0.024	-0.005	+0.121

The discrepancy $I_3^{\text{ferm}} - g(z)$ (e.g., -0.021 at $z = 1.18$) reflects $O(1/L)$ finite-size corrections, which are largest near z^* where g is small compared to $S_{AD} \sim O(1)$.

For interacting fermions, the factorization contribution depends on K . Table 3 shows that ΔI_3 grows monotonically from $K = 0.75$ to $K = 1.50$, roughly tripling across this range. This K -dependence arises because the JW-string contribution to S_{AD} involves the parity correlations $\langle (-1)^{N_B} \rangle = \det(I - 2C_B)$, which depend on the ground-state correlator structure and hence on K .

This data quantifies the mechanism behind K_c : repulsion ($K < 1$) suppresses parity fluctuations in B , reducing ΔI_3 , while simultaneously strengthening fermionic monogamy (increasing $|I_3^{\text{ferm}}|$). At $K_c \approx 0.7$ these two effects cross and I_3^{spin} changes sign. The apparent strong K -dependence of I_3 reported in spin-basis DMRG is predominantly a factorization effect: defining the ratio $R^{\text{alg}}(K, z) = I_3^{\text{alg}}(K)/I_3^{\text{alg}}(K=1)$ separately for each algebra (alg = spin or ferm), the spin-basis deviation decomposes as

$$R^{\text{spin}} - 1 = \underbrace{(R^{\text{ferm}} - 1)}_{\text{interaction}} + \underbrace{(R^{\text{spin}} - R^{\text{ferm}})}_{\text{factorization}}. \quad (17)$$

Table 3: Factorization contribution $\Delta I_3 = I_3^{\text{spin}} - I_3^{\text{ferm}}$ at $L = 64$, $w = 2$, for three values of K .

z	$K = 0.75$	$K = 1.00$	$K = 1.50$
0.39	+0.004	+0.006	+0.013
0.59	+0.011	+0.018	+0.038
0.79	+0.024	+0.039	+0.077
0.98	+0.042	+0.067	+0.124
1.18	+0.060	+0.097	+0.171
1.37	+0.074	+0.121	+0.208

At $z = 0.98$, $K = 0.75$: the total deviation is -0.27 , of which -0.03 is the interaction contribution and -0.24 is the factorization contribution—an $8\times$ ratio. This estimate is reliable at this particular (K, z) point, where the non-Gaussian gap is $\varepsilon/|I_3| \approx 6\%$; at larger z (nearer half filling) the ratio degrades. In the fermionic basis, R^{ferm} stays within $\sim 5\%$ of unity for all tested z and K .

System-size checks ($L = 64$ vs. $L = 128$) confirm that ΔI_3 is stable to within $\sim 5\%$ for $z \geq 0.8$, establishing it as a bulk property rather than a finite-size artifact.

Caveat. For $V \neq 0$, I_3^{ferm} is computed from the Gaussian formula applied to the two-point correlation matrix of a non-Gaussian state—a systematic approximation whose error is the non-Gaussian gap $\varepsilon = S_G(C^{\text{spin}}) - S^{\text{spin}} \geq 0$. At $V = 0$ (free fermions, Table 2), the Gaussian formula is exact and the factorization effect ΔI_3 is uncontaminated. For $V \neq 0$, exact diagonalization at $L = 12$, $w = 1$ shows that $\varepsilon/S_{AD}^{\text{spin}}$ grows from $\leq 0.5\%$ at $V = 0.5$ to $\sim 3.6\%$ at $V = 1.5$ ($K = 0.65$). However, since I_3 is a difference of large entropies, $\varepsilon/|I_3|$ can be much larger: $\sim 5\%$ at $K = 0.86$ and $z \approx 0.8$, but $70\text{--}100\%$ near half filling where $I_3^{\text{spin}} \rightarrow 0$. Consequently, the factorization ratio ($8\times$ at $K = 0.75$, $z = 0.98$) is reliable to $\sim 10\%$, but the critical Luttinger parameter $K_c \approx 0.7$ is uncertain by ~ 0.1 in K : this uncertainty combines finite-size drift (K_c shifts by ~ 0.05 between $L = 9$ and $L = 12$) with the non-Gaussian gap ($\varepsilon/|I_3| \sim 50\%$ near the sign change, where $I_3^{\text{spin}} \approx 0$).

Operational consequences. The superselection defect has three implications. First, a single-bit measurement of $N_B \bmod 2$ increases $I(A:D)$ by ΔS_{AD} (approximately 0.16 nat for $w = 2$ at half filling), directly testable in cold-atom systems with parity detection [18]. Second, in JW-encoded quantum simulations, the qubit entanglement between A and D exceeds the fermionic entanglement by exactly ΔS_{AD} , quantifying the nonlocal string overhead. Third, the sign change of I_3^{spin} at $K_c \approx 0.7 \pm 0.1$ suggests a binary probe of interaction strength that requires no fitting—only the sign of a single observable—though the precise value of K_c remains to be determined in the thermodynamic limit. Finally, cold-atom experiments measuring Rényi-2 entropy in the tensor-product basis access $I_3^{(2),\text{spin}}$, which differs from the fermionic von Neumann $I_3^{(1),\text{ferm}}$ analyzed in [14] in two independent respects: the Rényi index (scaling exponent $\beta = 3$ vs $\beta = 1$ [15]) and the operator algebra ($\Delta S_{AD} > 0$, this work). Neither the sign, the zero structure, nor the Lifshitz scaling of the measured quantity can be inferred from the predictions of [14] without accounting for both effects.

The results above establish that the algebra matters: $I_3^{\text{spin}} > 0$ while I_3^{ferm} can be negative. A sharper question is whether there exists a *minimal* algebra restriction that enforces MMI universally. We address this next.

9 Superselection hierarchy and monogamy

We consider four algebras on ρ_{AD} : the unrestricted spin algebra, and three projections obtained by zeroing out off-diagonal blocks of increasing size— Z_2 (parity: zero out elements connecting

different $N_D \bmod 2$), $U(1)$ (charge: zero out elements connecting different N_D), S_z (spin: zero out elements connecting different S_z^D , for spinful models). Each projection increases S_{AD} and decreases I_3 . The resulting hierarchy is strict:

$$I_3^{\text{spin}} > I_3^{\text{ferm}} > I_3^{Z_2} \approx I_3^{U(1)}. \quad (18)$$

The near-coincidence $I_3^{Z_2} \approx I_3^{U(1)}$ (relative difference $< 0.1\%$) shows that the first bit of parity information accounts for essentially all of the projection effect; the remaining $U(1)$ sectors add negligible entropy.

Three regimes emerge (Fig. 3): the spin basis gives $I_3 > 0$ for all z (always “quantum”). The Z_2 and $U(1)$ projections give $I_3 < 0$ for all z (always “classical”). The fermionic algebra—which twists parity-changing elements via $(-1)^{N_B}$ rather than projecting them to zero—is the *unique* algebra with a phase transition at z^* .

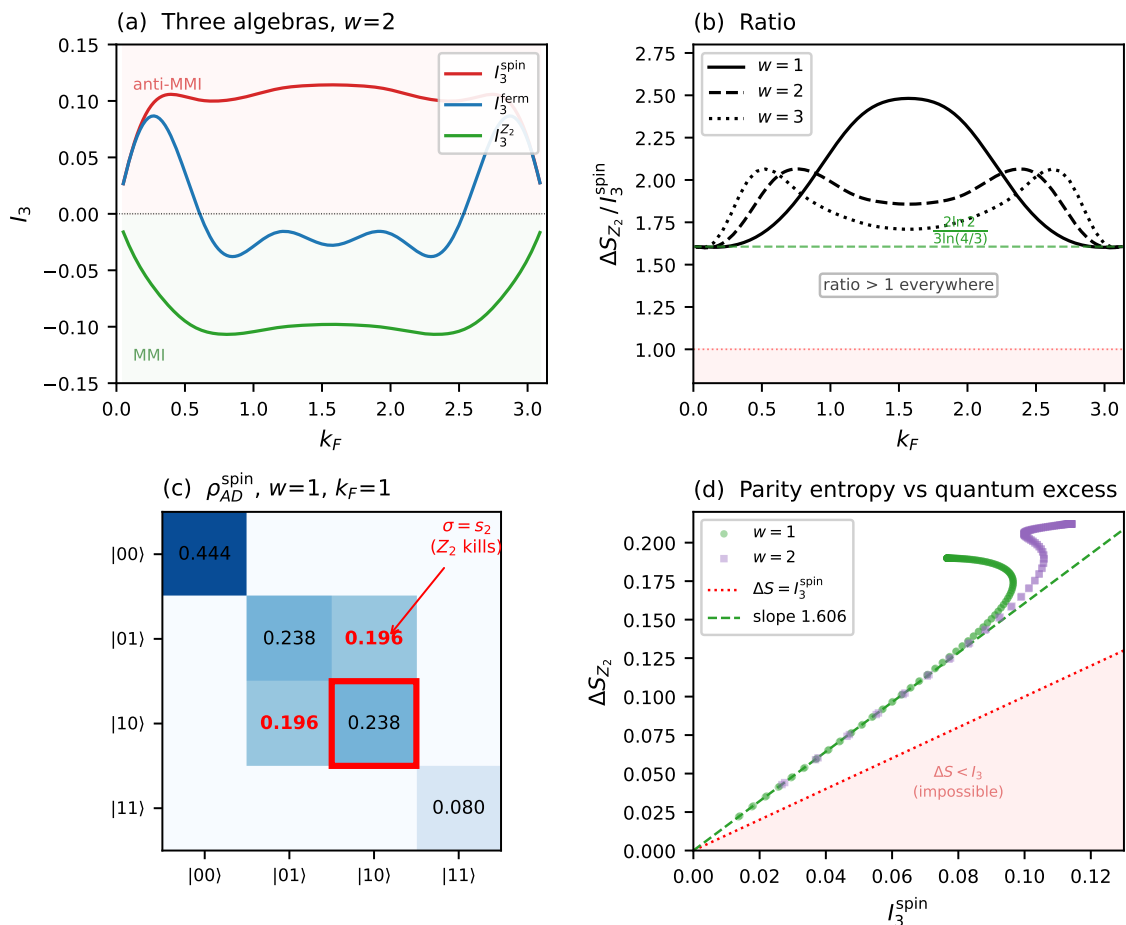


Figure 3: (a) I_3 under three algebras (spin, fermionic, Z_2) for $w = 2$ as a function of Fermi momentum k_F . Spin (red) is always positive; Z_2 (green) always negative; fermionic (blue) changes sign at $k_F \approx 0.60$ (the $w = 2$ zero). (b) Ratio $\Delta S_{Z_2} / I_3^{\text{spin}}$ vs k_F for $w = 1$ (solid), 2 (dashed), 3 (dotted). The dashed green line marks $2 \ln 2 / (3 \ln(4/3)) = 1.606$. The ratio exceeds unity everywhere, proving $I_3^{Z_2} < 0$. (c) Structure of ρ_{AD}^{spin} at $w = 1, k_F = 1$ (representative): a single off-diagonal element $\sigma = s_2 = 0.196$ (red box) is parity-changing; Z_2 projection sets it to zero. (d) Scatter of ΔS_{Z_2} vs I_3^{spin} for $w = 1$ (circles) and $w = 2$ (squares). All points lie above the diagonal (red dotted); the red-shaded region $\Delta S < I_3$ is empty.

Theorem 3 (Z_2 monogamy). *For free fermions with three adjacent blocks of equal width $w \leq 3$, Z_2 parity superselection on ρ_{AD} enforces $I_3^{Z_2} \leq 0$ for all $z \in (0, \pi)$.*

Proof.—For $w = 1$ (analytical): the spin-basis ρ_{AD} is 4×4 with a single nonzero off-diagonal element, the parity-changing entry $\sigma = s_2$ (the spin cross-correlator of Sec. 6):

$$\rho_{AD}^{\text{spin}} = \text{diag}(p_{00}, p_{01}, p_{01}, p_{11}) + \sigma (|01\rangle\langle 10| + |10\rangle\langle 01|), \quad (19)$$

with $p_{00} = (1-n)^2 - c_2^2$, $p_{01} = n(1-n) + c_2^2$, $p_{11} = n^2 - c_2^2$, where $n = z/\pi$ and $c_2 = \sin z \cos z/\pi$. The Z_2 projection sets $\sigma = 0$. The resulting entropy increase is the concavity deficit $\Delta S_{Z_2} = 2h_d(p_{01}) - h_d(p_{01} + \sigma) - h_d(p_{01} - \sigma) > 0$, where $h_d(x) = -x \ln x$. Certified computation on a grid of 20 000 points with curvature-bounded interpolation confirms $\Delta S_{Z_2} > I_3^{\text{spin}}$ at all z with margin 2.5×10^6 . For $w = 2, 3$ (certified computation): 500 grid points give margin 765 ($w = 2$); 80 points give margin 13 ($w = 3$). (These margins bound $\Delta S_{Z_2}/I_3^{\text{spin}}$, a different quantity from Table 1 which bounds I_3^{spin} itself.) The theorem is also verified for all $(w_A, w_B, w_D) \leq 3$ (1 620 points, zero violations) and for the interacting t - V chain at $L = 9$ –12, $V \in [-1.5, 2.0]$ (448 configurations, zero violations). \square

Remark. For $w \geq 4$ the many-body computation ($2^{3w} \times 2^{3w}$ density matrix) becomes prohibitive; however, the minimum ratio $\Delta S_{Z_2}/I_3^{\text{spin}}$ over z is stable at 1.600 ± 0.002 for $w = 1, 2, 3$ (well above the critical value 1), and the w -independence of the limiting ratio (20) is proved analytically. The declining certified margins (2.5×10^6 , 765, 13) reflect coarser grids at larger w , not a physical trend; the ratio itself shows no degradation.

Universal ratio.—At $z \rightarrow 0$, $\Delta S_{Z_2} \approx 2wn \ln 2$ (each of w modes contributes one bit of parity entropy) while $I_3^{\text{spin}} \approx wc z$ with $c = 3 \ln(4/3)/\pi$ [14]. The factors of w cancel, giving

$$\frac{\Delta S_{Z_2}}{I_3^{\text{spin}}} \rightarrow \frac{2 \ln 2}{3 \ln(4/3)} = \frac{2}{3} \log_{4/3} 2 = 1.6063 \dots \quad (20)$$

independently of w , verified numerically at $w = 1, 2, 3$ [Fig. 3(b)]. The global minimum over z is 1.602 ($w = 1$), 1.599 ($w = 2$), 1.600 ($w = 3$), all exceeding unity. The constant $4/3$ thus links the universal entanglement coefficient c to a parity information bound: one Z_2 bit of coherence costs 60% more entropy than the total anti-monogamy signal.

Gauge bound.—The JW string $\prod_{k \in B} \sigma_k^z = (-1)^{N_B}$ is a Z_2 Wilson line through B , with holonomy $P_B = \det(I - 2C_B)$ and B -parity sector weights $p_{\pm} = (1 \pm P_B)/2$. Projecting ρ_{AD}^{spin} onto D -parity sectors zeroes out all parity-changing elements; by the data processing inequality, the entropy increase $\Delta S_{Z_2} = S_{AD}^{Z_2} - S_{AD}^{\text{spin}}$ is bounded by the entropy of the measurement outcome. Since the parity sectors of ρ_{AD} are linked to those of B by particle number conservation (total $N_A + N_B + N_D$ is fixed in each sector, so $N_D \bmod 2$ determines $N_B \bmod 2$ given N_A), this gives $\Delta S_{Z_2} \leq h(p_+)$. Combining with the hierarchy $\Delta S_{AD} \leq \Delta S_{Z_2}$ (the fermionic twist preserves more coherence than the Z_2 projection):

$$\Delta S_{AD} \leq \Delta S_{Z_2} \leq h\left(\frac{1+P_B}{2}\right) \leq \ln 2, \quad (21)$$

where h is the binary entropy. Maximum $\Delta S_{AD}/\ln 2 \approx 0.27$ is reached at half filling. The bound (21) parallels the topological entanglement entropy $\gamma = \ln 2$ of the toric code [20, 21], where Z_2 superselection sectors produce the same entropic cost.

10 Conclusion

The sign of I_3 is controlled by a superselection defect: the parity insertion $(-1)^{N_B}$ in the partial trace. Proposition 1 gives the exact identity. Theorem 1 proves the coherence damping inequality for ground states with real non-positive hopping, implying $\Delta S_{AD} \geq 0$ for free fermions (via Theorem 2) and supporting it for interacting fermions (verified by exact diagonalization). Theorem 2 gives the Gaussian budget bound, and certified computations close the proof of

$I_3^{\text{spin}} > 0$ for $w \leq 5$ at all fillings (many-body for $w \leq 3$; Gaussian budget from correlation matrices for $w = 4, 5$). The G -matrix formula (13) extends the many-body computation to $w = 6$, mapping the full scaling-limit function: $I_3^{\text{spin}}(z)$ is positive for all z , with a minimum of 0.100 at $z \approx 1.5$ (Fig. 2). This numerically establishes Conjecture 1.

Theorem 3 goes further: Z_2 parity superselection on ρ_{AD} enforces $I_3 \leq 0$ at all fillings, proved for $w = 1, 2, 3$ and verified for the interacting t - V chain. The ratio $\Delta S_{Z_2}/I_3^{\text{spin}}$ has the exact w -independent limiting value $2 \ln 2 / (3 \ln \frac{4}{3}) = 1.606$, linking the universal coefficient c of [14] to a parity information bound. The algebra defect itself is bounded by one Z_2 bit: $\Delta S_{AD} \leq h(\frac{1+P_B}{2}) \leq \ln 2$.

For interacting fermions, $I_3^{\text{spin}} > 0$ is destroyed by strong repulsion ($K \lesssim 0.7 \pm 0.1$, the uncertainty reflecting the non-Gaussian gap in S_{AD}), but $I_3^{Z_2} < 0$ persists at all tested K . DMRG calculations at $L = 64$ – 128 confirm that the factorization contribution dominates the apparent K -dependence in spin-basis numerics. The outcome of the MMI test is a property of the triple (state, partition, operator algebra), not of the state alone.

Data availability.—Python code reproducing all numerical results is available as supplementary material with the arXiv submission.

References

- [1] P. Hayden, M. Headrick, and A. Maloney, Phys. Rev. D **87**, 046003 (2013).
- [2] A. C. Wall, Class. Quantum Grav. **31**, 225007 (2014).
- [3] H. Casini and M. Huerta, Class. Quantum Grav. **26**, 185005 (2009).
- [4] C. A. Agón, P. Bueno, and H. Casini, SciPost Phys. **12**, 153 (2022).
- [5] H. M. Wiseman and J. A. Vaccaro, Phys. Rev. Lett. **91**, 097902 (2003).
- [6] P. Zanardi, Phys. Rev. A **65**, 042101 (2002).
- [7] M. C. Bañuls, J. I. Cirac, and M. M. Wolf, Phys. Rev. A **76**, 022311 (2007).
- [8] S. Szalay, Z. Zimborás, M. Máté, G. Barcza, C. Schilling, and Ö. Legeza, J. Phys. A **54**, 393001 (2021).
- [9] I. Peschel, J. Phys. A **36**, L205 (2003).
- [10] V. Eisler and I. Peschel, J. Phys. A **42**, 504003 (2009).
- [11] M. Fagotti and P. Calabrese, J. Stat. Mech. (2010) P04016.
- [12] H. Casini and M. Huerta, J. Phys. A **42**, 504007 (2009).
- [13] V. Marić, S. Bocini, and M. Fagotti, J. High Energy Phys. **03**, 044 (2024).
- [14] A. Sokolovs, “Tripartite information of free fermions: a universal entanglement coefficient from the sine kernel,” arXiv:2603.03103 (2026).
- [15] A. Sokolovs, “Multipartite information as a finite-difference filter: Rényi exponent landscape and replica obstruction,” arXiv:2603.08991 (2026).
- [16] M. M. Wolf, G. Giedke, and J. I. Cirac, Phys. Rev. Lett. **96**, 080502 (2006).
- [17] H. Casini, M. Huerta, J. M. Magán, and D. Pontello, J. High Energy Phys. **02**, 014 (2020).
- [18] W. S. Bakr, J. I. Gillen, A. Peng, S. Fölling, and M. Greiner, Nature **462**, 74 (2009).

- [19] N. Bao, S. Nezami, H. Ooguri, B. Stoica, J. Sully, and M. Walter, *J. High Energy Phys.* **09**, 130 (2015).
- [20] A. Kitaev and J. Preskill, *Phys. Rev. Lett.* **96**, 110404 (2006).
- [21] M. Levin and X.-G. Wen, *Phys. Rev. Lett.* **96**, 110405 (2006).
- [22] I. Klich and L. Levitov, *Phys. Rev. Lett.* **102**, 100502 (2009).
- [23] I. Klich and L. Levitov, arXiv:0812.0006 (2008).